Experimental verification of numerical thin film evaporation model

Jakub Devera[1,*], Tomáš Hyhlík[1]

[1] CTU in Prague, Faculty of Mechanical Engineering, Technická 4, 166 07 Praha 6, Czech Republic

Abstract

The report deals with experiment with an objective to verify the correctness of fluid film evaporation numerical model. The First part is about selection and description of chosen method. The Second part is concerning with a design of test rig. For a primary concept, the mathematical model respecting conservation of mass and energy was developed. Further, the construction design and used measurement devices are described. The last part is related to validation of the test rig and checking if all the requirements taken into consideration in the design and in numerical model are fulfilled.

Keywords: evaporation, experiment, humidity, fluid film

1. Introduction

A usage of CFD simulation in developing or improving technical applications expanded very quickly in many industrial fields. Many applications deal with an evaporation of thin fluid film. At The Department of Fluid Dynamics and Thermodynamics, a numerical model based on an analogy between heat and mass transfer was developed. The output of the model is a calculation of the evaporation time of the fluid film of given thickness.

To validate and verify the CFD model a test rig had to be designed. Figuring out the method of measuring liquid film thickness was the first objective. The description of major methods is written below.

1.1. Measuring of liquid film thickness

The original intention of numerical model verification was measuring directly the liquid film thickness and its depletion during evaporation. Evaluated evaporation rate would be compared with results from the numerical model.

The easiest and straightforward method is a usage of a needle-contact sensor mounted on a stand with a micrometric traverser. The one-point measuring in whole fluid film area is the problem of this method. Also, another obstacle is negative impact of the traverser on the flow around the traverser. This method is usually used for the calibration of sophisticated methods. [1]

Another technique is an interferometric optic method. A laser beam is reflected from the liquid surface and the solid surface and the interfering reflected beams are captured by high-speed CCD camera. If the fluid film includes particles, it also can be used laser scattering technique. The amount of light scattered by the particles is dependent on the film thickness. [2] [3]

The conductance method is based on a potential difference between electrodes and measuring resulting current. The conductivity between the electrodes is dependent on the film thickness between them. [4]

1.2. Measuring of relative humidity change

After doing a research in the liquid film thickness measuring techniques, a different attitude was chosen. Instead of measuring liquid film thickness and evaluating evaporation rate, it was decided to measure a change of relative humidity of air flow while passing a mixing area with a film with constant temperature. Vapor evaporating from the film is saturating the air flow, so relative humidity is changing. A difference of humidity at the outlet and the inlet of the mixing area will be measured.

For this type of measuring, a test rig with specific requirements has to be designed. One of the requirements laminar flow with uniform velocity profile in the mixing area. A further requirement is keeping a constant temperature of the fluid film during the measurement. For simplifying the problem, the water film thickness will be considered as constant too. Then, it is possible to look at this problem as a stationary problem.

According to the geometry of the test rig, the numerical film evaporation model will be updated and the results of the both method will be compared.

2. Design of the test rig

2.1. Mathematical model

The elemental dimensions of the test rig have to be designed to respect to the measurable change of relative humidity. To determine the dimensions, a mathematical model was developed. The model is based on conservation of mass

$$\dot{m}_a(1 + x_{in}) + \dot{m}_w = \dot{m}_a(1 + x_{out}) \qquad (1)$$

* Kontakt na autora: Jakub.Devera@fs.cvut.cz

and energy

$$\dot{Q} + \dot{m}_a (h_{1+x})_{in} + \dot{m}_a (1 + x_{in}) \frac{v_{in}^2}{2} \dot{m}_w h_v(t_w) = \dot{m}_a (h_{1+x})_{out} + \dot{m}_a (1 + x_{out}) \frac{v_{out}^2}{2} \qquad (2)$$

in a control volume shown in figure 1:

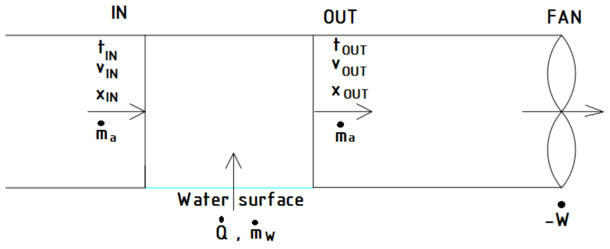

Fig. 1. *Balanced control volume.*

Equation (1) can be rewritten to form (3), where is clear, that the difference of specific humidity depends on the ratio of mass flow rates $\dot{m}_a, \dot{m}_w$.

$$\frac{\dot{m}_w}{\dot{m}_a} = x_{out} - x_{in} \qquad (3)$$

where:

$$\dot{m}_w = \beta \cdot A_{WS}\big(\rho''_{wv}(t_w) - \rho_{wv}(t_{in})\big) \qquad (4)$$

$$\dot{m}_a = v \cdot \rho_a \cdot A_{duct} \qquad (5)$$

In equations (4) and (5) only t_{in} and ρ_a are set by laboratory conditions. The rest of physical quantities can be thought as optional parameters (the velocity of the flow t_w, the temperature of the fluid film surface t_w, the area of the cross-section of mixing part A_{duct} and the area of the water surface A_{WS}). The mass transfer coefficient β is defined as follows:

$$\beta = \frac{D \cdot Sh}{L} \qquad (6)$$

D (the diffusion coefficient), Sh (the Sherwood number) and L is a function of fluid properties and parameters discussed above. The mass transfer coefficient was solved using criterion equations. The Sherwood number for mass exchange at the surface of a flaw plate considering forced convection and laminar flow [5]

$$Sh = 0.646 Re^{1/2} Sc^{1/3} \qquad (7)$$

where Re is the Reynolds number and Sc is the Schmidt number.

The diffusion coefficient of a water vapor was calculated using equation [6]

$$D_{wv} = \frac{0.926}{1000 \cdot p} \cdot \frac{t_{in}{}^{2.5}}{t_{in} + 245} \qquad (8)$$

where p is the atmospheric pressure.

Dependencies of inlet, outlet and saturated specific humidity were plotted. These diagrams were used to determine the optimal value of each parameter. The selected values of the parameter are highlighted in the diagrams.

From diagram (fig.2) , the inlet mass flow rate was determined as $\dot{m}_a = 9{,}74$ g/s. Given the assumption of laminar flow in the mixing area and keeping the calm surface of the fluid film, the velocity of the flow was chosen as $v = 0{,}1 m/s$. The area of cross-section of the mixing part $A_{duct} = 0{,}081 m^2$ was calculated from these values.

From diagram (fig.3), the length of the film surface was determined as $L = 0{,}5 m$, from diagram (fig.4), the temperature of the water film was obtained.

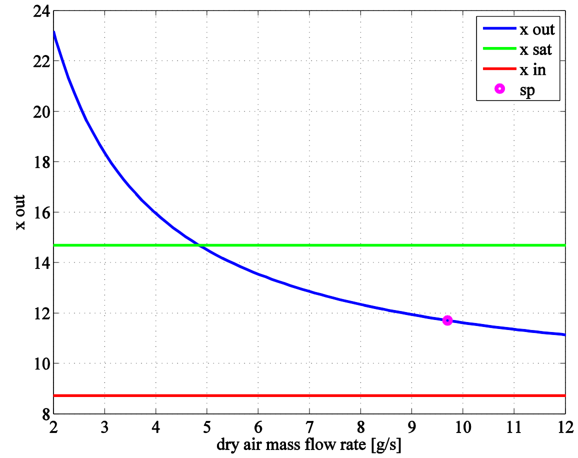

Fig. 2. *Dependency of inlet, outlet and saturated specific humidity on the dry mass flow rate*

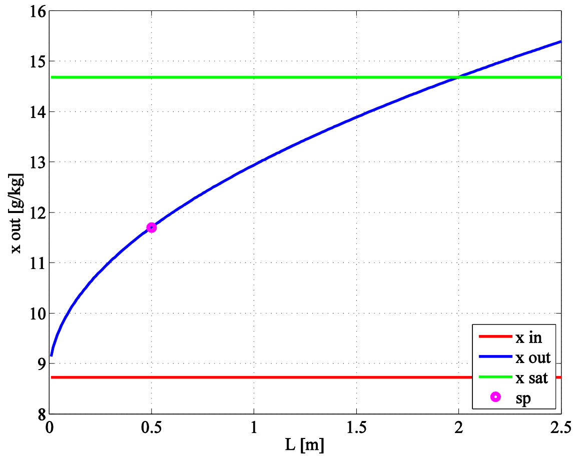

Fig. 3. *Dependency of inlet, outlet and saturated specific humidity on the water surface length*

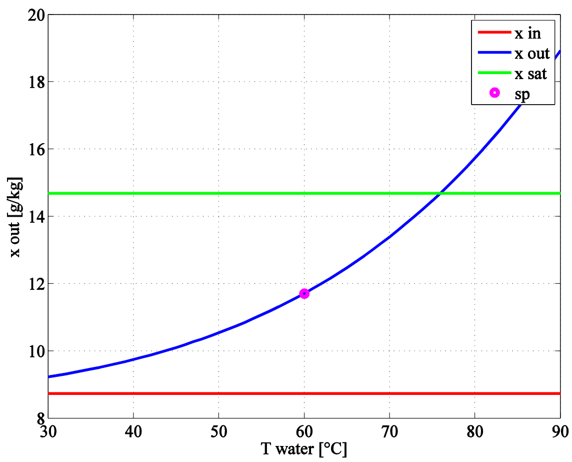

Fig. 4. *Dependency of inlet, outlet and saturated specific humidity on the temperature of water*

If the cross-section area doesn't change, it is possible to consider the difference of inlet and outlet kinetic energy as negligible:

$$\dot{Q} + \dot{m}_a (h_{1+x})_{in} - \dot{m}_w h_v(t_w) = \dot{m}_a (h_{1+x})_{out} \quad (9)$$

At the place, where the outlet relative humidity will be measured, the humidity profile has to be uniform. If the laminar flow during the mixing area is considered, the flow won't be mixed and the profile will be nonuniform. This fact leads to an idea to measure the outlet humidity behind a fan propelling the test rig which the flow mixes. Due to measuring the relative humidity by a psychrometer, an affecting wet and dry bulb temperature by a fan performance is necessary to take into consideration:

$$\dot{Q} + \dot{W} + \dot{m}_a (h_{1+x})_{in} - \dot{m}_w h_v(t_w) = \dot{m}_a (h_{1+x})_{out} \quad (10)$$

To calculate the temperature difference caused by the fan performance, the humidity component is neglected and equation (10) can be rewritten to form:

$$\dot{m}_a\, c_p\, t_{fan-in} = \dot{m}_a\, c_p\, t_{fan-out} - \dot{W} \quad (11)$$

2.2. Construction design

Based on previous calculations a construction design of test rig was made. The design has to meet the requirements discussed above:

- Uniform velocity profile in the mixing area
- Uniform and constant temperature profile of the fluid film
- Uniform humidity profile at the point of measuring outlet humidity

The design is shown in figure 5. Uniform velocity profile is secured by a nozzle. In the mixing area, a water tank is located which used as a container of heated water to keeping constant temperature of the water film. The film is created by dipping an aluminum plate to the water tank. The water tank is heated by heating foils located at sides and bottom of the tank. The performance of foils can be regulated so the constant temperature of the water can be kept. At the bottom side of the aluminum plate, digital thermometers are mounted to monitor the temperature profile of the plate. The plate is thick enough so it is possible to consider the temperature of the plate as the temperature of the water film. The water tank was designed to be replaceable so it is possible to change the length of water surface from 0.5m to 1.0 m.

The area of cross-section of the mixing part was calculated as $A_{duct} = 0{,}081 m^2$, in the test rig, the square cross-section of dimensions 0,3m x 0,3m is used with $A_{duct} = 0{,}090 m^2$. The mixing part is made of plexiglass so PIV method to measure velocity field of the flow inside the mixing area can be used. Built test rig is shown in figure 6.

Fig. 6. *Photo of the test rig*

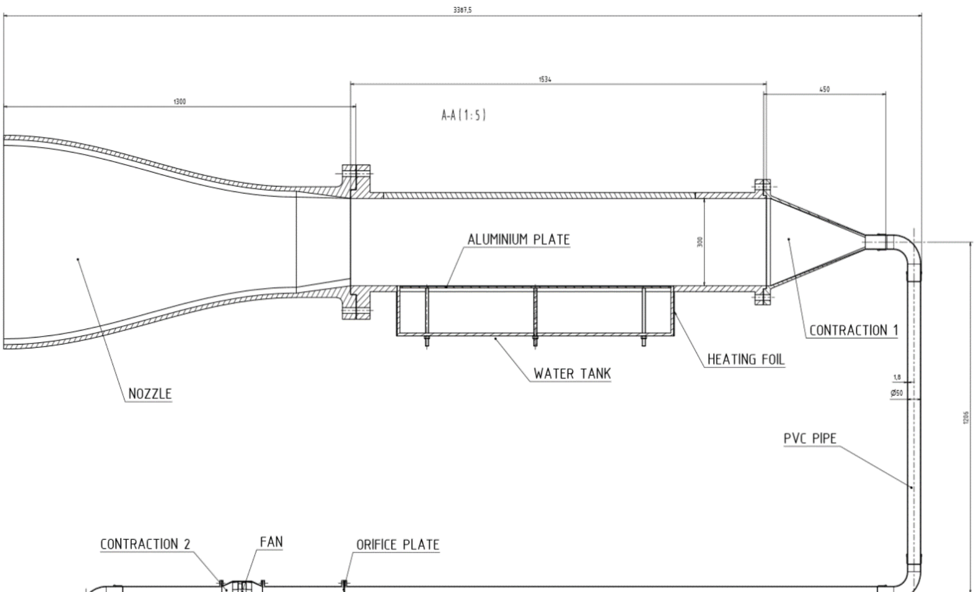

Fig. 5. *The design of the test rig*

At the end of the mixing part, the square to round transition is used. Between pipe flanges, an orifice plate meter is embedded which is used to measure mass flow rate of the air flow. The orifice meter is devices for reducing static pressure. The mass flow rate is proportional to pressure lost so it can be calculated from the pressure difference in front of and behind the orifice:

$$\dot{m}_a = \dot{q}_m \approx C \cdot \varepsilon \cdot \sqrt{\Delta p} \qquad (12)$$

The coefficient of discharge C is also a function of $\dot{q}_m$ so the calculation of $\dot{q}_m$ has to run iteratively. ε is an expansibility factor, which depends on dimensions of orifice and pipeline and on the pressure difference. The orifice meter was designed by iso standard, so standardized equations are used to calculation the coefficients. Two differential pressure sensors are used for the measuring the pressure loss. One is installed for measuring the pressure difference of orifice plate (range 125 Pa), the second one is measuring the pressure difference between the front side of the orifice and the atmospheric pressure.

Behind the orifice, a fan is propelling the test rig and mixing the air flow. Relative humidity of mixed flow is calculated from a temperature difference of dry bulb and wet bulb temperature measured by device called a psychrometer which is inserted in a pipe. The psychrometer consists of two temperature sensors connected to printed circuit board and it is own design by Department of Fluid Dynamics and Thermodynamics. The temperature difference is tabulated so relative humidity can be easily expressed.

3. Validation verification

3.1. Verification of uniform velocity profile

Particle Image Velocimetry (PIV) is modern method of flow visualization using seeding particles in examining fluid, which is illuminated by a laser beam so that particles are visible. The light beam is converted to a line by a cylindrical lens, so a selected plane of a physical area can be illuminated and recorded by CCD camera. A 2D velocity field can be reconstructed from a digitized data from the camera.

Several planes of the mixing area will be inspected to evaluate the uniformity of velocity profile. A deviation between velocity field from each plane will be calculated. Also, measured velocity field will be compared with velocity field in matching plane from the numerical simulation. The middle cross-section of velocity field from the numerical simulation is shown in figure 7.

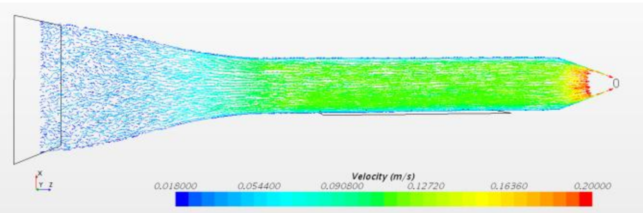

Fig. 7. *Simulated velocity field inside the mixing area in middle cross-section*

3.2. Sensitivity of humidity difference on water film thickness

Second validation measurement is testing the rig for different water film thickness in order to determine the sensitivity of humidity difference on film thickness. It is worked with an assumption that film thickness doesn't have an effect on evaporation rate and it is not necessary to keep uniform thickness during the whole humidity measurement. To confirm this assumption, three measurements with various film thickness will be realized as shown below in figure 8.

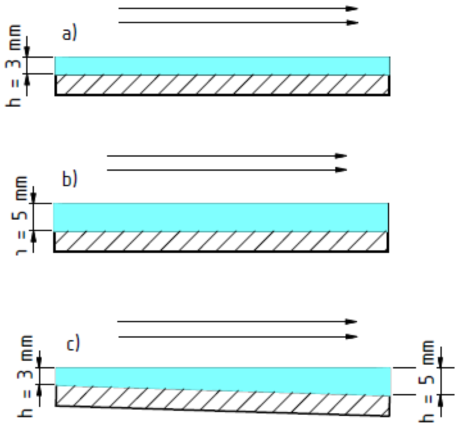

Fig. 8. *Different set of water film thickness during the measurement (a: 3mm, b: 5mm, c: linear change from 3mm to 5mm)*

4. Conclusion

This report briefly summarizes methods of direct measuring of water film thickness. Then a method of measuring a difference of relative humidity is introduced. The method is based on a change of humidity of air flowing above water film.

The mathematical model of the test rig was developed to design dimension of the test rig. The model respects conservation of mass and energy. The choice of dimensions was chosen from dependencies of inlet, outlet and saturated specific humidity on dry mass flow rate, the length and the temperature of the water film.

In the next part of this paper, the main construction requirements are said (uniform velocity profile in the mixing area, uniform and constant temperature profile of fluid film and uniform humidity profile at the point of measuring outlet humidity) and how they were technically solved. Measuring devices are also covered.

The test rig has to be validated before the start of measuring so two validation measurement were proposed (verification of uniform velocity profile and sensitivity of humidity difference on water film thickness). Because the test rig is in the process of validation now, results from the measurement are not available yet.

Nomenclature

A	area (m^2)
C	coefficient of discharge (1)
c_p	specific heat capacity ($J \cdot kg^{-1} \cdot K^{-1}$)
D	mass diffusivity ($m^2 \cdot s^{-1}$)
h	water film thickness (m)
h	enthalpy ($J \cdot kg^{-1}$)
h_{1+x}	moist air enthalpy ($J \cdot kg^{-1}$)
L	length of the water surface (m)
$\dot{m}$, $\dot{q}_m$	mass flow rate ($kg \cdot s^{-1}$)
p	pressure (Pa)
Δp	pressure difference (Pa)
$\dot{Q}$	heat flux (W)
Re	Reynolds number (1)
Sc	Schmidt number (1)
Sh	Sherwood number (1)
t	temperature (K)
v	velocity ($m \cdot s^{-1}$)
$\dot{W}$	fan performance (W)
x	specific humidity ($kg \cdot kg^{-1}$)
β	mass transfer coefficient ($m \cdot s^{-1}$)
ε	expansibility factor (1)
ρ	density ($kg \cdot m^{-3}$)
ρ"	saturation density ($kg \cdot m^{-3}$)
a	dry air
w	water
ws	water vapor
in	inlet
out	outlet

Literature

[1] LU Q., SURYANARAYANA N. V. a CHRISTODOULU C. Film thickness measurement with an ultrasonic transducer. Experimental Thermal and Fluid Science [online]. 1993, **7**(4), 354-361 [cit. 2016-04-10]. Accessible from: http://linkinghub.elsevier.com/retrieve/pii/089417779390058Q

[2] BORGETTO, N., GALIZZI C., ANDRÉ F. a ESCUDIÉ D. A thickness measurement technique based on low-coherence interferometry applied to a liquid film with thermal gradient. Experimental Thermal and Fluid Science [online]. 2010, 34(8), 1242-1246 [cit. 2016-04-10]. Accessible from: http://linkinghub.elsevier.com/retrieve/pii/S0894177710001068

[3] GRESZIK, D., YANG H., DREIER T. a SCHULZ C. Measurement of water film thickness by laser-induced fluorescence and Raman imaging. Applied Physics B [online]. 2011, **102**(1), 123-132 [cit. 2016-04-10]. Accessible from: http://link.springer.com/10.1007/s00340-010-4200-x

[4] CONEY, M W E. The theory and application of conductance probes for the measurement of liquid film thickness in two-phase flow. Journal of Physics E: Scientific Instruments [online]. 1973, **6**(9), 903-911 [cit. 2016-04-10]. Accessible from: http://stacks.iop.org/0022-3735/6/i=9/a=030?key=crossref.666d1f376c723fe54e0fa4fd4f0569f3

[5] PERRY R. H., GREEN D. W. Perry's chemical engineers' handbook. 7th ed. /. New York: McGraw-Hill, c1997.

[6] KRÖGER, D. G. Air-cooled heat exchangers and cooling towers: thermal-flow performance evaluation and design. Volume II. Tulsa, Okla.: PennWell, 2004.